JVI Journals.ASM.org

Conserved Neutralizing Epitope at Globular Head of Hemagglutinin in H3N2 Influenza Viruses

Yoshitaka Iba,[a] Yoshifumi Fujii,[b]* Nobuko Ohshima,[a] Tomomi Sumida,[b]* Ritsuko Kubota-Koketsu,[c] Mariko Ikeda,[b]* Motoaki Wakiyama,[b]* Mikako Shirouzu,[b]* Jun Okada,[d] Yoshinobu Okuno,[e] Yoshikazu Kurosawa,[a] Shigeyuki Yokoyama[b]*

Institute for Comprehensive Medical Science, Fujita Health University, Toyoake, Aichi, Japan[a]; RIKEN Systems and Structural Biology Center, Suehiro, Tsurumi, Yokohama, Japan[b]; Department of Virology, Research Institute for Microbial Diseases, Osaka University, Suita, Osaka, Japan[c]; Sales and Marketing Division, Medical and Biological Laboratories Co., Ltd., Nagoya, Aichi, Japan[d]; Kanonji Institute, The Research Foundation for Microbial Diseases, Osaka University, Kanonji, Kagawa, Japan[e]

ABSTRACT

Neutralizing antibodies that target the hemagglutinin of influenza virus either inhibit binding of hemagglutinin to cellular receptors or prevent the low-pH-induced conformational change in hemagglutinin required for membrane fusion. In general, the former type of antibody binds to the globular head formed by HA1 and has narrow strain specificity, while the latter type binds to the stem mainly formed by HA2 and has broad strain specificity. In the present study, we analyzed the epitope and function of a broadly neutralizing human antibody against H3N2 viruses, F005-126. The crystal structure of F005-126 Fab in complex with hemagglutinin revealed that the antibody binds to the globular head, spans a cleft formed by two hemagglutinin monomers in a hemagglutinin trimer, and cross-links them. It recognizes two peptide portions (sites L and R) and a glycan linked to asparagine at residue 285 using three complementarity-determining regions and framework 3 in the heavy chain. Binding of the antibody to sites L (residues 171 to 173, 239, and 240) and R (residues 91, 92, 270 to 273, 284, and 285) is mediated mainly by van der Waals contacts with the main chains of the peptides in these sites and secondarily by hydrogen bonds with a few side chains of conserved sequences in HA1. Furthermore, the glycan recognized by F005-126 is conserved among H3N2 viruses. F005-126 has the ability to prevent low-pH-induced conformational changes in hemagglutinin. The newly identified conserved epitope, including the glycan, should be immunogenic in humans and may induce production of broadly neutralizing antibodies against H3 viruses.

IMPORTANCE

Antibodies play an important role in protection against influenza virus, and hemagglutinin is the major target for virus neutralizing antibodies. It has long been believed that all effective neutralizing antibodies bind to the surrounding regions of the sialic acid-binding pocket and inhibit the binding of hemagglutinin to the cellular receptor. Since mutations are readily introduced into such epitopes, this type of antibody shows narrow strain specificity. Recently, however, broadly neutralizing antibodies have been isolated. Most of these bind either to conserved sites in the stem region or to the sialic acid-binding pocket itself. In the present study, we identified a new neutralizing epitope in the head region recognized by a broadly neutralizing human antibody against H3N2. This epitope may be useful for design of vaccines.

Influenza is an infectious disease of the respiratory tract that affects millions of people every year. Antibodies (Abs) are important for protection against influenza virus infection, and hemagglutinin (HA) is the main target for virus-neutralizing Abs. HA mediates virus entry into cells at two steps (1). First, HA binds to the cell receptor, sialic acid. After internalization of viruses by endocytosis, HA undergoes a marked conformational change induced by low pH, resulting in fusion between the virus envelope and cell membrane. Since the sialic acid-binding pocket and its surrounding regions are immunogenically potent, the majority of neutralizing Abs induced by virus infection or vaccination binds to these regions and prevents the binding of HA to sialic acid. This activity is experimentally measured by hemagglutination inhibition (HI) assay. Historically, the epitopes recognized by these neutralizing Abs have been mapped by isolation of escape mutants. The epitopes present on the globular head of HA are well characterized, and they are clustered in five sites: A, B, C, D, and E in HA of H3 viruses (2, 3) and Sa, Sb, Ca_1, Ca_2, and Cb in HA of H1 viruses (4). Because mutations are readily introduced into these sites without losing receptor-binding activity, variant viruses that have acquired resistance to these Abs become dominant and cause

Received 11 February 2014 **Accepted** 3 April 2014

Published ahead of print 9 April 2014

Editor: T. S. Dermody

Address correspondence to Yoshikazu Kurosawa, kurosawa@fujita-hu.ac.jp.

Y.I. and Y.F. contributed equally to this article.

* Present address: Yoshifumi Fujii, RIKEN Structural Biology Laboratory, Suehiro, Tsurumi, Yokohama, Japan; Tomomi Sumida, RIKEN Structural Biology Laboratory, Suehiro, Tsurumi, Yokohama, Japan; Mariko Ikeda, RIKEN Center for Life Science Technologies, Suehiro, Tsurumi, Yokohama, Japan; Motoaki Wakiyama, RIKEN Center for Life Science Technologies, Suehiro, Tsurumi, Yokohama, Japan; Mikako Shirouzu, RIKEN Center for Life Science Technologies, Suehiro, Tsurumi, Yokohama, Japan; Shigeyuki Yokoyama, RIKEN Structural Biology Laboratory, Suehiro, Tsurumi, Yokohama, Japan.

Supplemental material for this article may be found at http://dx.doi.org/10.1128/JVI.00420-14.

doi:10.1128/JVI.00420-14

The authors have paid a fee to allow immediate free access to this article.

annual epidemics. Thus, while preventive vaccination has been the most efficient measure of influenza control, the vaccine strains need to be changed almost every year to remain effective (5).

In 1993, Okuno et al. isolated mouse monoclonal Ab (MAb) C179, which has broad neutralization activity against group 1 viruses, including H1N1, H2N2, and H5N1 (6, 7). These researchers found that C179 recognizes the conserved sequences 318 to 322 of HA1 and 47 to 58 of HA2, which are located in the middle of the HA stem region, and prevents virus infection by inhibiting HA-mediated membrane fusion. Recently, this conclusion was directly confirmed by X-ray analysis of the crystal structure of C179 in complex with H2 HA (8). Fifteen years later, three groups independently isolated human MAbs that broadly neutralized group 1 viruses (9–11). Abs neutralized both H1N1 and H5N1 viruses, and they utilized the V_H1-*69* gene. Structural analyses of HA-Ab complexes of two clones, CR6261 and F10, by X-ray crystallography further indicated that the Abs block infection by inserting their heavy (H) chain into a conserved pocket in the stem region and blocking conformational rearrangements of HA, thus preventing membrane fusion (11, 12). Two amino acids in the complementarity-determining region (CDR) 2, isoleucine at residue 53 and phenylalanine at residue 54, are found only in the human V_H1-*69* gene and play an essential role in the HA-Ab interaction. Recently, three broadly neutralizing Abs, which prevent the low-pH induced conformational change in HA, were isolated from humans as follows: CR8020 against group 2 viruses (13), FI6 against group 1 and 2 viruses (14), and CR9114 against influenza A and B viruses (15). X-ray analyses of crystal structures of the HA-Ab complexes revealed that they also recognize highly conserved regions in the HA stem. In addition to the broadly neutralizing Abs against the HA stem, several groups isolated broadly neutralizing Abs that bind to the globular head (15–23). If the Abs target the sialic acid-binding pocket itself, they could show broad neutralization activity; there have been reports of such Abs (16–23). In two cases, CH65 and C05, long peptides in the CDR3 of H chain were directly inserted into the sialic acid-binding pocket and formed stable complexes, generating strong binding activity (16–18). An epitope conserved in all H1N1 viruses was identified between the sialic acid-binding pocket and site Ca_2. MAb 5J8, which binds to this epitope, has HI activity (19, 20). CR8033, another MAb that broadly neutralizes influenza viruses, binds to a region close to the sialic-acid-binding pocket (15).

We also isolated broadly neutralizing Abs by screening a phage-display library made from a large number of B lymphocytes which were collected by apheresis from a healthy donor born in 1974 (24). The collection of neutralizing Abs contained two types of clone that had broad strain specificity. The first type neutralized not only H3N2 but also H1N1, H2N2, and H5N1 viruses, although the activities varied markedly. Our data suggested that the sialic acid-binding pocket is part of the epitope recognized by this type of clone, F045-092. The second type bound to all 12 H3N2 viruses but not to group 1 viruses. In the present study, we determined the epitope recognized by one of these Abs, F005-126, and the mechanism by which it neutralizes the viruses.

MATERIALS AND METHODS

Viruses. For experiments and analyses, we used one A/H1N1 strain, A/New Caledonia/20/1999 (NC99), and the following A/H3N2 strains: A/Aichi/2/1968 (Aic68), A/Fukuoka/1/1970 (Fuk70), A/Tokyo/6/1973 (Tok73), A/Yamanashi/2/1977 (Yam77), A/Niigata/102/1981 (Nii81), A/Fukuoka/C29/1985 (Fuk85), A/Guizhou/54/1989 (Gui89), A/Kitakyushu/159/1993 (Kit93), A/Sydney/5/1997 (Syd97), A/Panama/2007/1999 (Pan99), A/Wyoming/3/2003 (Wyo03), and A/New York/55/2004 (NY04). In addition to these strains, the amino acid sequences of HA in the following strains were used for analyses: A/H1N1 strains A/South Carolina/1/1918 (SC1918) and A/California/04/2009 (Cal09pdm), A/H2N2 strain A/Japan/305+/1957 (Jpn57), A/H5N1 strain A/Viet Nam/1203/2004 (Viet04), A/H7N3 strain A/Turkey/Italy/214845/2002 (aviIta02), and A/H9N2 strain A/swine/Hong Kong/9/98 (swHK98). Abbreviations for the strains are shown in parentheses. The A/H3N2 strains listed above, NC99 and Cal09pdm, have been used for influenza vaccines in Japan.

Construction of Ab library. A large combinatorial Ab library was constructed using the phage-display method, as described previously (25, 26). Briefly, 1.3×10^9 B lymphocytes from a healthy donor born in 1974 were collected by apheresis from the equivalent of 3 l of blood. From B lymphocytes, heavy (H) and light (L) chain libraries were constructed, which contained 3.7×10^9 and 1.6×10^8 clones, respectively. Finally, H and L chains were combinatorially assembled. The resulting Ab library contained 2.9×10^{10} clones.

Screening of Ab library. Phages bound to virus particles were selected by a panning method as described previously (24). Briefly, formalin-treated virus particles were used as antigens (Ags) in the screening of the phage Ab library containing 2.9×10^{10} clones. After panning three times, eluted phages were used to infect *Escherichia coli* DH12S. Infected *E. coli* was spread onto Luria-Bertani plates containing 100 μg of ampicillin/ml and 0.2% glucose. Colonies were picked up, and *E. coli* cells harboring phagemid were grown in 2×YT medium containing 100 μg of ampicillin/ml, 0.05% glucose, and 1 mM IPTG (isopropyl-β-D-thiogalactopyranoside) at 30°C overnight. The Fab-cp3 form of MAb was secreted into medium (27). Culture supernatants containing Fab-cp3 molecules were subjected to enzyme-linked immunosorbent assay (ELISA) against 12 H3N2 strains and an H1N1 NC99 strain of influenza viruses. Clones that were bound to H3 but not to NC99 were selected and subjected to sequencing for classification. The amino acid positions of VH and VL were coordinated according to Kabat numbering by using the AbNum server (28).

Preparation of MAbs. Phagemid DNAs from isolated MAb clones were digested with SalI and then self-ligated to convert the Fab-cp3 form into the Fab-PP form (29). The Fab-PP Abs (P denotes a single Fc-binding domain of protein A) were secreted into medium after induction with IPTG, as described above, and were purified with IgG-Sepharose (GE Healthcare). The IgG form of F005-126 was prepared as described previously (30) (GenBank accession numbers AB848924 for H chain and AB848925 for L chain) and was purified with protein A-Sepharose (GE Healthcare).

Neutralization assay. Neutralizing activity was measured by focus reduction assay as described previously (31). A series of dilutions of F005-126 IgG (50 μl) was mixed with 100 PFU of influenza virus (50 μl) and was then applied to monolayers of MDCK cells in 96-well microplates. After culture for 6 h, the cells were fixed with ethanol and incubated with mouse anti-influenza NP antibody C43 and then rabbit anti-mouse IgG antibody (Cappel), followed by goat anti-rabbit IgG antibody. Finally, cells were incubated with peroxidase and rabbit anti-peroxidase complex (Cappel). Infected cells were stained with 3,3′-diaminobenzidine tetrahydrochloride. The data are expressed as the percentage reduction rate in infected cells.

HI assay. Serial dilutions of 100 μg of purified F005-126 IgG/ml in phosphate-buffered saline (PBS) were preincubated with 4 HA units of virus per well. Guinea pig red blood cells were added to a final concentration of 0.5%, and the plate was incubated at room temperature for 30 to 60 min.

Isolation of escape mutants. Escape mutants were isolated by incubating Aic68 strain with IgG1 Ab using a previously described method (32) with some modification. Briefly, 10^5 focus-forming units of virus/ml

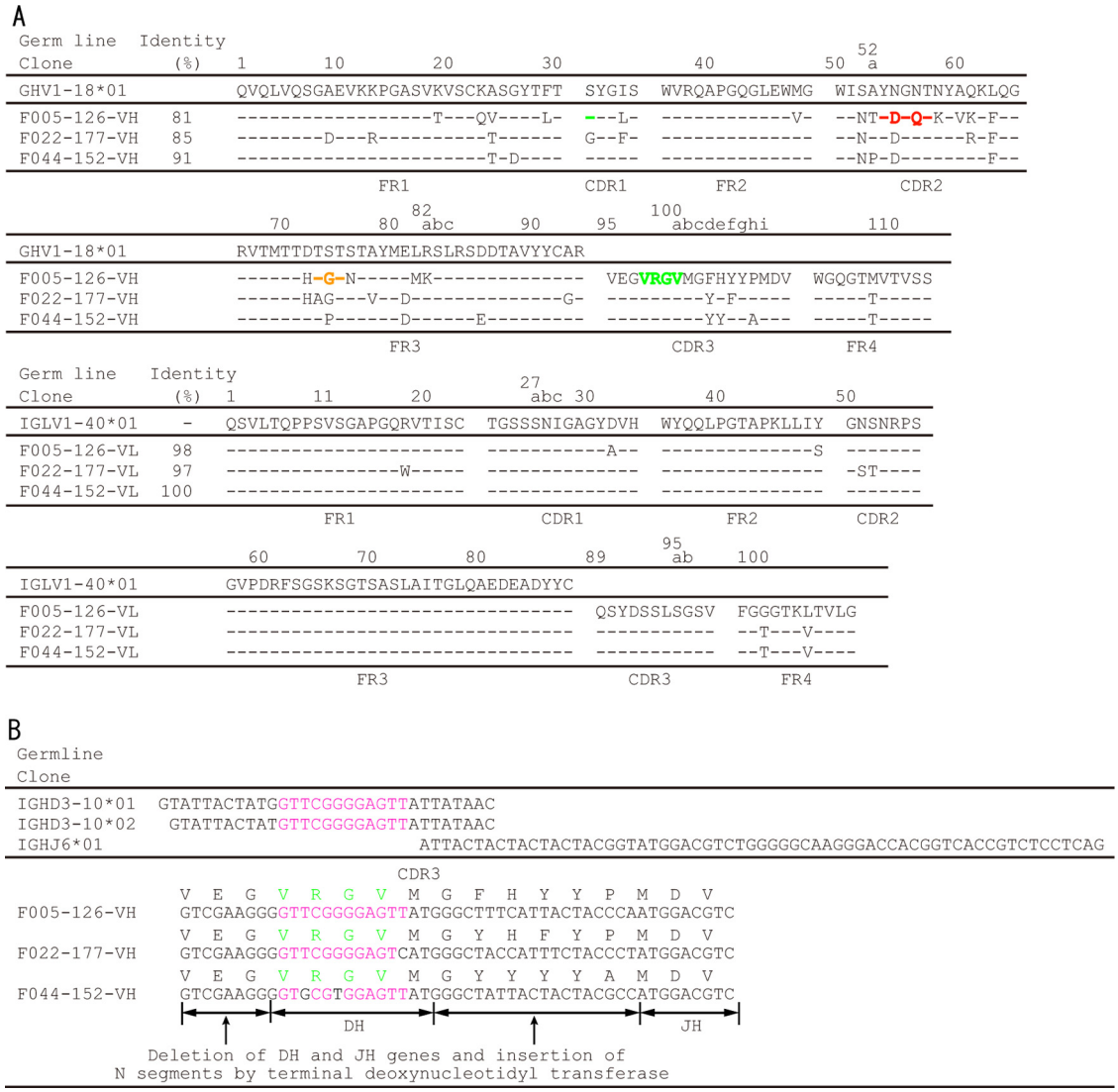

FIG 1 Amino acid sequences of F005-126 VH and VL. (A) Amino acid numbers are according to the Kabat numbering system. Framework regions FR1, FR2, FR3, and FR4 and complementary determining regions CDR1, CDR2, and CDR3 are shown. Comparison of amino acid sequences of VHs and VLs to germ line sequences was performed according to IgBLAST (http://www.ncbi.nlm.nih.gov/igblast/). Amino acid sequence identities (%) of MAbs with germ line VH or VL are shown. From X-ray analysis, amino acid sequences indicated in orange, green, and red were bound to site L, site R, and a glycan at HA-R:Asn285, respectively. (B) Predicted deletion of D_H and J_H genes and insertion of N segments are shown. The nucleotide sequence GTTCGGGGAGTT, encoding the 4-amino-acid sequence V98–R99-G100–V100a in F005-126–HCDR3, is indicated in pink.

were incubated at 37°C for 1 h in the presence of 5 μg of Ab. Virus-Ab mixture was added to MDCK cells in 24-well plates and incubated at 35°C for 3 days. Neutralization tests on each well were performed separately with Abs to identify the escape mutants. The nucleotide sequence of escape mutants was determined using the following primers: H3HA forward, 5′-GCAAAAGCAGGGGATAATTCT; H3HA backward, 5′-GTAGAAACAAGGGTGTTTTTAATTA; and H3HA 568, 5′-TGAACGT GACTATGCCAAACAATG.

Construction of plasmid DNAs for cell surface expression of HA and HA1 domain. DNAs encoding Fuk85 HA ectodomain (residues 1 to 513), Fuk85 HA1 domain (residues 1 to 329), and NC99 ectodomain (residues 1 to 513) were amplified by PCR and inserted into the KpnI-ApaI sites in pYD1 (Invitrogen), resulting in HA and derivatives connected with a V5 epitope tag. DNAs encoding HA and derivatives with a V5 tag were again amplified by PCR and were inserted into SfiI-SalI sites in pDisplay (Invitrogen). The resultant plasmid DNAs encode a V5 tag between the transmembrane region (transmembrane domain of PDGFR) and the extracellular domain of HA and derivatives. The resultant plasmid DNAs encode a V5 tag between the HA ectodomain or HA1 domain and the PDGFR transmembrane domain.

Flow cytometry (FCM) analysis of 293T cells expressing HA on cell surface. 293T cells in a 150-mm dish were transiently transfected with 24 μg of plasmid DNA expressing HA or no DNA (mock transfection) mixed with 60 μl of Lipofectamine LTX (Invitrogen). Cells were recovered after culture in Dulbecco modified Eagle medium (Wako) at 37°C for 24 h and blocked with 2.5% bovine serum albumin in PBS on ice. Cells were then incubated with 5 μg of IgG Ab/ml, 10 μg of Fab-PP Ab/ml, 1 μg of mouse anti-H3 MAb F49 (33)/ml, or 1 μg of rabbit anti-V5 antibody (Millipore)/ml. Finally, cells were incubated with Alexa Fluor 488-labeled anti-human IgG, Alexa Fluor 488-labeled anti-mouse IgG, or Alexa Fluor 488-labeled anti-rabbit IgG (Molecular Probes), respectively, and subjected to FCM analysis.

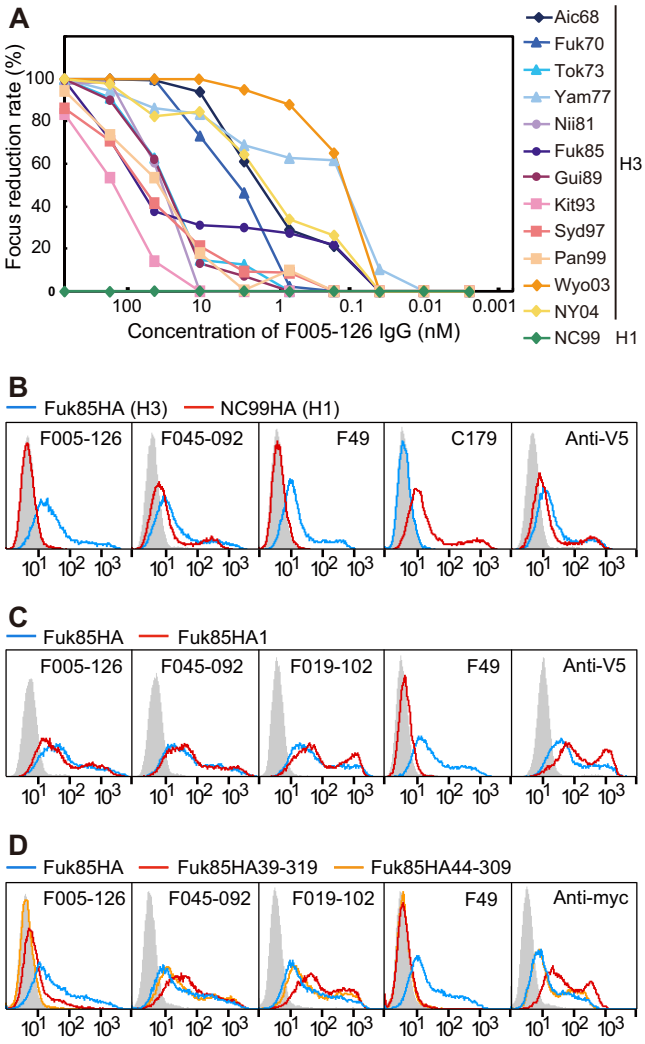

FIG 2 Neutralizing and binding activities of F005-126. (A) Virus-neutralizing activity against 12 H3N2 strains was measured by focus reduction assay (31). (B) Binding activity of Abs to HA artificially expressed on cells was examined by flow cytometry (FCM). Blue line, HA of Fuk85 (H3N2); red line, HA of NC99 (H1N1); gray filled, mock transfection. F045-092 binds to both H3-type and H1-type HAs (24). F49 binds to an epitope on HA2 commonly present in H3 HA (33). C179 binds to the stem region of HA of group 1 virus. Anti-V5 Ab binds to the V5 tag located at the membrane-proximal end of HA. (C) Binding activity of Abs to HA (blue) and HA1 domain (red) of Fuk85 was analyzed by FCM. F019-102 binds to site E on HA1 (35). (D) Binding activity of Abs to HA (blue) and truncated HAs, HA39-319 (red) and HA44-309 (orange) of Fuk85 was analyzed by FCM. Anti-myc Ab binds to the myc tag located at the membrane-proximal end of HA.

FCM analysis of 293T cells expressing two types of truncated HA. DNAs encoding Fuk85 HA regions corresponding to residues 44 to 309 and residues 39 to 319 were amplified by PCR and inserted into the ApaI-SalI sites in pDisplay. The resultant plasmid DNAs encode truncated Fuk85 HAs with a myc tag between the truncated HA and a PDGFR transmembrane domain. Truncated HAs were expressed on 293T cells and subjected to FCM analyses. Expression of truncated HAs was verified by detecting HAs on cells by mouse anti-myc tag antibody (MBL).

FCM analysis of 293T cells expressing mutant Aic68HA/N285Y. DNA encoding Aic68HA ectodomain (residues 1 to 513) from A/Aichi/2–1/1968 (H3N2) strain (accession number AB847411) was amplified by PCR and inserted into the ApaI-SalI sites in pDisplay to give Aic68HA/wild type. DNA encoding a mutant Aic68HA/N285Y in which asparagine at 285 in HA1 was changed into tyrosine was inserted into the same sites in pDisplay. Aic68HA/wild-type and Aic68HA/N285Y were expressed on 293T cells, and the cells were subjected to FCM analysis.

Competitive ELISA. We performed competitive ELISA for F005-126 and four MAbs that had been isolated previously (34). The epitopes recognized by these four MAbs were successfully assigned to one of five sites on the globular head that had been well characterized as neutralizing epitopes (35). Competitive ELISA was performed using Fab-PP as the primary Ab to detect binding to virus particles and Fab-cp3 as a competitor. Fab-PP is Fab fused with IgG-binding domain of protein A, and Fab-cp3 is Fab fused with coat protein 3 (cp3) of filamentous phage. Fab-cp3 molecules in the supernatant of *E. coli* culture were concentrated 20-fold. Fab-PP of F005-126, F045-092, F041-342, F041-360, F019-102, and F037-115 (24, 34) were purified. Formalin-inactivated H3N2 (Yam77) virus particles were coated onto a MaxiSorp immunoplate. A total of 50 μl of Fab-PP at an optimized concentration was mixed with 50 μl of 20-fold-concentrated Fab-cp3 and added to a virus-coated immunoplate. Peroxidase-conjugated rabbit Ab, which binds to IgG-binding domain of protein A in Fab-PP, was then added. Finally, *o*-phenylenediamine was added, and the optical density at 492 nm was measured.

Protein expression and purification. For preparation of HA trimer for crystallography, we used the gene encoding HA from A/Aichi/2–1/1968 (H3N2) strain (accession number AB847411). The ectodomain of Aic68 HA (residues 1 to 504) was cloned into expression vector pBAC-3, as C-terminal fusions with a thrombin protease cleavage site, a trimerization "foldon" sequence, and His tag (accession number AB849024). Fusion proteins were synthesized using a baculovirus expression system. During incubation at 27°C for 48 h, HA protein was secreted into culture medium. Cell debris was removed by centrifugation at 3000 × *g* for 20 min, and the supernatant was concentrated using the QuickStand system (GE Healthcare). Concentrated culture supernatant was then loaded onto a HisTrap column (5 ml; GE Healthcare) pre-equilibrated with buffer A (10 mM Tris-HCl [pH 8.0] containing 500 mM NaCl, 5% glycerol, 20 mM imidazole). The column was washed with 50 ml of buffer A, and HA was eluted with 10 mM Tris-HCl (pH 8.0) containing 500 mM NaCl, 5% glycerol, and 500 mM imidazole. Fractions were pooled and dialyzed against 20 mM Tris-HCl (pH 8.0) and 20 mM NaCl containing thrombin protease to cleave the His tag. To separate the His tag and uncleaved protein, protein was loaded onto a HisTrap column, and flowthrough fractions were collected. Protein was further purified by ion exchange on a HiTrap Q column (5 ml; GE Healthcare) and size exclusion chromatography on a HiLoad 16/60 Superdex 200-pg column (GE Healthcare) in final buffer containing 20 mM Tris-HCl (pH 8.0) and 150 mM NaCl. IgG form of F005-126 was incubated with immobilized papain (Pierce), and Fab fragments generated by papain digestion were separated from undi-

TABLE 1 Neutralizing activity and HI activity of F005-126[a]

Strain	IC_{50} (nM)	HI
A/Aichi/2/1968 (H3N2)	1.4	ND
A/Fukuoka/1/1970 (H3N2)	3.1	–
A/Tokyo/6/1973 (H3N2)	29	–
A/Yamanashi/2/1977 (H3N2)	0.12	ND
A/Niigata/102/1981 (H3N2)	36	–
A/Fukuoka/C29/1985 (H3N2)	71	ND
A/Guizhou/54/1989 (H3N2)	29	–
A/Kitakyushu/159/1993 (H3N2)	157	–
A/Sydney/5/1997 (H3N2)	64	ND
A/Panama/2007/1999 (H3N2)	41	ND
A/Wyoming/3/2003 (H3N2)	0.12	ND
A/New York/55/2004 (H3N2)	1.3	–
Aichi68/N285Y mutant	49	–
A/New Caledonia/20/1999 (H1N1)	ND	–

[a] ND, activity was not detected; –, not tested.

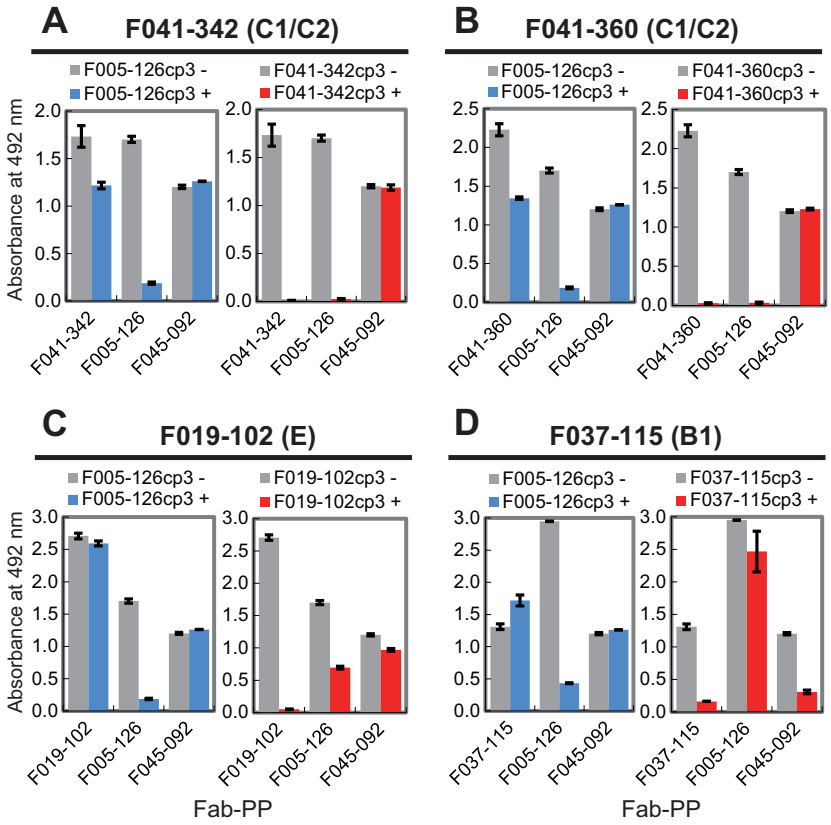

FIG 3 Competition for binding to HA between F005-126 and four MAbs that bind to sites C1/C2, E, and B1 on HA1. Competitive ELISA for Yam77 virus particles was performed by using Fab-PP as primary Ab for detection of binding activity without (−) (gray) or with (+) (red or blue) a large excess of competitor Fab-cp3 (for example, F041-342cp3). Fab-PP is Fab fused with IgG-binding domain of protein A, and Fab-cp3 is Fab fused with coat protein 3 (cp3) of filamentous phage. Fab-PP was detected by peroxidase-conjugated rabbit Ab. The antigenic sites recognized by the four MAbs—F041-342, F041-360, F019-102, and F037-115—are indicated in parentheses above the graphs.

gested IgG and Fc fragments by chromatography on a HiTrap rProteinA FF column (GE Healthcare). For crystallization of the HA-Fab complex, HA and Fab were mixed in a 1:1.2 molar ratio and incubated at 4°C overnight. HA-Fab complex was separated from uncomplexed proteins by chromatography on a HiLoad 16/60 Superdex 200-pg column that was preequilibrated with 20 mM Tris-HCl (pH 8.0)–150 mM NaCl. Fractions containing complex proteins were pooled and concentrated to 10 mg/ml with an Amicon-15 filter (Millipore).

Crystallization and X-ray data collection. The initial screening of crystallization conditions was conducted with commercially available screening kits (Hampton Research). The HA-Fab complex crystals were obtained in crystallization conditions using the sitting-drop vapor diffusion method with polyethylene glycol (PEG) as the precipitant. Crystals were obtained in a few days by mixing 1 μl of sample solution and 1 μl of reservoir solution containing 12% PEG8000, 0.2 M KCl, 0.1 M $Mg(CH3COO)_2$, and sodium citrate buffer (pH 5.5). For diffraction data collection, crystals were soaked in reservoir solution containing 20% glycerol. The data sets were collected with the BL41XU beamline at SPring-8 (Hyogo, Japan).

Data collection, structure determination, and refinement. Diffraction data were collected at 100K on the BL41XU beamline at SPring-8. Diffraction images were processed with XDS (36) and HKL2000 (37). The structure was solved at 4.0-Å resolution by molecular replacement (MR) with PHASER using the structures of H3 (PDB 1HA0) and Fab (PDB 1EO8) (38, 39) as starting models. CH1/CL domains in Fabs curved in the different patterns because the Fab elbow linking variable and constant domains is flexible (22). Since a clear electron density map appeared at

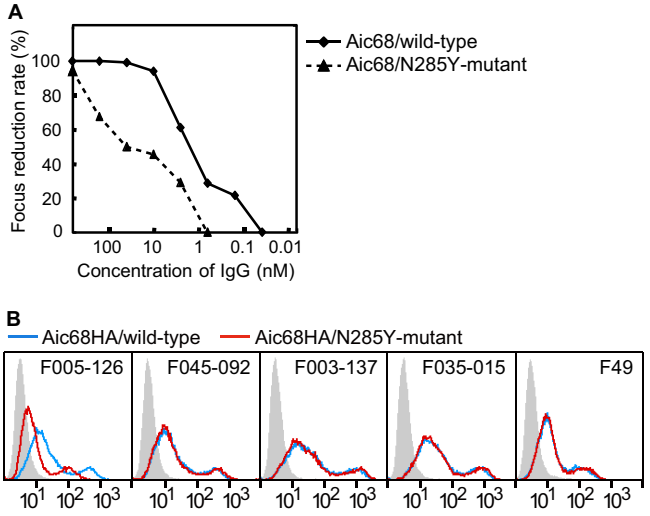

FIG 4 Neutralization and binding activity of F005-126 against mutant Aic68/N285Y. (A) Neutralization activity of F005-126 against an escape mutant, Aic68N285Y, was weaker than that against the wild-type Aic68 strain. (B) FCM analyses of the cells expressing Aic68HA/wild-type and a mutant Aic68HA/N285Y were performed. FCM signals for mock transfection (gray filled), wild-type HA-expressing cells (blue), and mutant HA-expressing cells (red) are shown. F045-092, F003-137, and F035-015 recognize the HA head region (24, 34). Binding activity of F005-126 to Aic68HA/N285Y was weaker than that to wild-type HA.

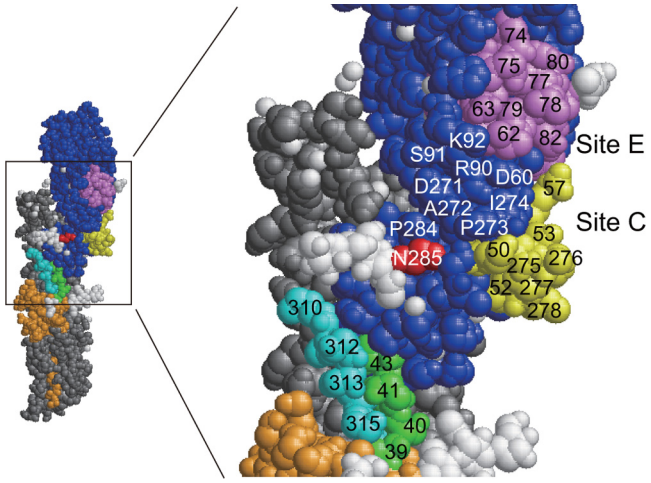

FIG 5 Amino acids around site C, site E, and Asn285 in HA1 on the 3D structure of H3 HA. Residues 50 to 57 and residues 275 to 279 in antigenic site C are indicated in yellow. Residues 62 to 83 in antigenic site E are indicated in violet. Residues 39 to 43, 310 to 316, and 285 in HA1 are indicated in green, cyan, and red, respectively. Residues 9 to 38 and residues 317 to 329 in HA1 are indicated in orange. Residues 44 to 309 are indicated in blue. The HA2 domain is gray. A glycan at Asn285 is white.

different positions from initial models, we judged that MR was successful. The asymmetric unit contains 4 HA trimers and 12 F005-126 molecules, and the structure was refined using CNS with tight restrains and manual rebuilding with Coot (40). Although the structure was solved at 4.0-Å resolution, noncrystallographic symmetry (NCS) averaging between 12 molecules and B-factor sharpening brought dramatic map improvement up to atomic resolution level (41, 42). To confirm our model quality, we compared over 10 Fab structures from wwPDB which have the highest sequence identities to F005-126, particularly at CDRs. All 12 VH/VL domains contact HA in the same manner, but CH1/CL domains show five curve types depending on crystal packing. Positive density for N-linked glycans was observed at five of the six predicted sites on HA, and a total of 20 sugar residues were built. Hydrogen bonds and van der Waals contacts between F005-126 and H3 HA were calculated using Contact (in CCP4) and MorProbity (43). The surface area buried upon Fab binding was calculated with MS (44). PyMol (DeLano Scientific) was used to render structure figures and for general manipulations. Final refinement statistics are summarized in Table 2.

Protease susceptibility assay. A protease susceptibility assay was performed as described previously (45). Briefly, purified Aic68HA and Fab-PP form of F005-126 (2.5 Fabs per HA protomer) were mixed in 50 mM Tris-HCl (pH 8.0) containing 1% dodecylmaltoside. The pH was lowered to 5.0 by adding 0.1 M sodium citrate (pH 2.5) to all samples except controls. Reaction mixtures were incubated at 25°C for 20 min, and the pH was neutralized by the addition of 1 M Tris-HCl (pH 8.9). Trypsin was added to all samples (except controls) at a final molar ratio of 1:100 (trypsin-HA), and samples were digested at 25°C for 40 min. Nonreducing sodium dodecyl sulfate (SDS) buffer was added to each reaction, followed by boiling for 5 min. Samples were subjected to SDS-PAGE, 0.63 μg of HA was applied to each lane, and gels were stained with Coomassie brilliant blue.

Nucleotide sequence accession numbers and protein data accession number. The nucleotide sequences of Abs and HA were deposited in the DDBJ database under accession numbers AB848924 for F005-126 H chain, AB848925 for F005-126 L chain, AB914707 for F022-177 H chain, AB914708 for F022-177 L chain, AB914709 for F044-152 H chain, AB914710 for F044-152 L chain, and AB847411 and AB849024 for the HA of A/Aichi/2–1/1968 (H3N2). Atomic coordinates and structure factors were deposited in the Protein Data Bank (PDB ID 3WHE).

RESULTS

Location of epitope recognized by F005-126. Among the clones isolated in our previous study, three clones in group 11 bound to all 12 H3N2 strains but did not bind to the H1N1 strain (24). The amino acid sequences of the V_H and V_L fragments of these clones are shown in Fig. 1A. The nucleotide sequence GTTCGGGGA GTT, encoding a 4-amino-acid sequence from Val98 to Val100a in F005-126–HCDR3, could be derived from the D_H gene *IGHD3-10*01* or *IGHD3-10*02* (Fig. 1B). The IgG form of F005-126 was prepared, and the neutralizing activity was measured by focus reduction assay (31). Although the Ab neutralized all 12 H3N2 strains with activities ranging from 0.12 to 157 nM (50% inhibitory concentration [IC_{50}]), it did not have any detectable HI activity (Fig. 2A and Table 1). In order to identify the location of the epitope, three experiments were performed as follows. In the first experiment, various forms of HA were artificially expressed on cells, and HA-Ab interaction was examined by FCM. When HA of H3N2 (Fuk85) and HA of H1N1 (NC99) were expressed on cells, F005-126 bound only to cells expressing HA of H3N2 (Fig. 2B). When HA and HA1 of H3N2 (Fuk85) were expressed on cells, F005-126 bound equally to HA and HA1 (Fig. 2C). The HA1 do-

TABLE 2 X-ray data collection and refinement statistics

Parameter	F005-126–H3 complex[c]
Data collection statistics	
Beamline	BL41XU
Wavelength (Å)	1.00
Space group	C2
Unit cell dimensions	
a, *b*, *c* (Å)	391.04, 241.17, 223.21
α, β, γ (°)	90.0, 123.62, 90.0
Resolution (Å)	40–4.0 (4.25–4.00)
Observations	554,887
No. of unique reflections	142,111 (23,528)
Redundancy	3.9 (3.9)
Completeness (%)	98.0 (98.1)
CC 1/2[a] (%)	99.9 (27.1)
Avg $I/\sigma I$	6.4 (1.26)
R_{merge}	0.23 (2.09)
Z ac	12
Refinement statistics	
Resolution range (Å)	40–4.0
R_{work} (free)	0.31 (0.33)
No. of atoms	
Protein	85,260
Carbohydrate	2,664
Water	0
B-factor	
Protein	170
Carbohydrate	196
RMSD[b]	
Bond length (Å)	0.004
Bond angle (°)	1.02
Ramachandran plot (%)	
Favored regions	93.9
Outliers	0.9
PDB ID	3WHE

[a] CC 1/2, percentage of correlation between intensities from random half-datasets (60).
[b] RMSD, root mean square deviation.
[c] Numbers in parentheses denote outer-shell statistics.

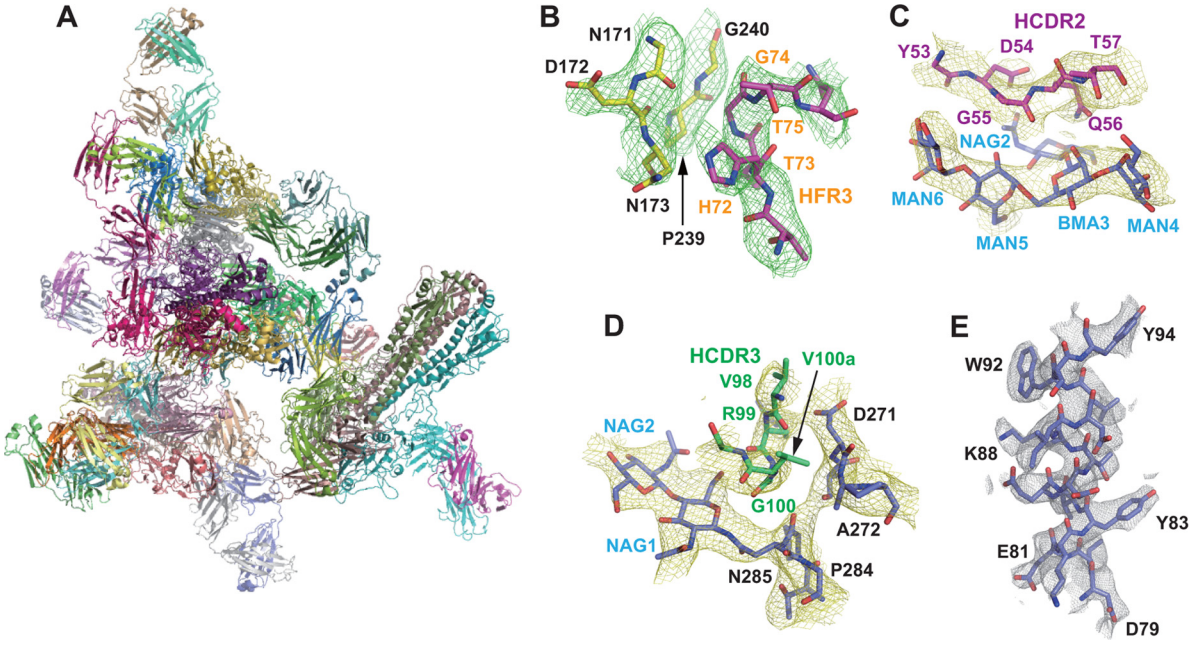

FIG 6 Crystal structure of F005-126 Fab in complex with Aic68/HA. (A) One HA trimer forms a complex with three F005-126 Fabs as indicated. In an asymmetric unit (AU), the crystal contains 12 F005-126 Fabs and four Aic68/HA trimers (twelve Aic68/HA monomers). Three Fabs bind to the HA trimer in the same manner. CH1/CL domains in 12 Fabs curve in the different patterns. (B to E) The figures show 2Fo-Fc electron density maps of the helix of residues 79 to 94 in HA2 (B), FR3 (C), CDR3 (D), and CDR2 (E). Fo means observed structure factor and Fc means calculated structure factor. The electron density is contoured at 1.5 σ and shown by a 12-fold noncrystallographically averaged map.

main contains 329 amino acid residues and is structurally divided into the globular head region (residues 39 to 319) and the stem region (residues 1 to 38 and 320 to 329). Regions consisting of residues 39 to 43 and residues 310 to 319 are closely associated in three-dimensional (3D) structure and are located at a junction between the head and stem regions (46). Two types of truncated HA, Fuk85HA39-319 (residues 39 to 319) and Fuk85HA44-309 (residues 44 to 309), were expressed on cells in order to examine the binding of F005-126. Figure 2D shows that F045-092, which binds to the sialic acid-binding pocket, and F019-102, which binds to site E (24, 35), bound well to the both truncated HAs, indicating that the 3D structure near the sialic acid-binding pocket is properly formed by the truncated HAs. F005-126 bound weakly to Fuk85HA39-319 but not to Fuk85HS44-309. Thus, the epitope recognized by F005-126 should be located on the globular head, apart from the sialic acid-binding pocket. Indeed, F005-126 did not possess HI activity. In the second experiment, competition of binding to HA was performed between F005-126 and various Abs with known epitopes (35). Both F041-342 and F041-360, which bind to site C, completely inhibited the binding of F005-126 to Yam77 HA (Fig. 3A and B). F019-102, which binds to site E, partly inhibited the binding of F005-126 (Fig. 3C). In contrast, F037-115, which binds to site B, did not inhibit the binding of F005-126 (Fig. 3D). These results suggest that the epitope recognized by F005-126 is located in the region adjacent to sites C and E but distant from site B. In the third experiment, an escape mutant was isolated in the presence of F005-126. Although a completely resistant variant could not be isolated, a partly resistant variant from Aic68 virus was present (Fig. 4A and Table 1). In this variant, asparagine at residue 285 in HA1 was mutated to tyrosine. We constructed a mutant with N285Y and expressed HA. As shown in Fig. 4B, the binding activity of F005-126 to the mutant HA was markedly weakened. Since asparagine at this residue is glycosylated, this mutation should result in deglycosylation. The relative positions of site C, site E, and residue 285 on the 3D structure of HA are shown in Fig. 5. All of these observations suggest that the epitope is located in a region near or partly overlapping sites C and E and that glycosylated Asn at residue 285 could be directly involved in forming the epitope.

Structural characteristics of F005-126 Fab-Aic68/HA complex. To examine the structural basis of F005-126 recognition, the crystal structure of F005-126 Fab in complex with Aic68/HA was solved at 4.0-Å resolution by molecular replacement with PHASER (Table 2). The structure was refined by using CNS with tight restrains and manual rebuilding with Coot (40). Because an asymmetric unit (AU) contains four HA trimers (twelve HAs) and 12 F005-126 Fabs (Fig. 6A), it was difficult to improve the resolution limit. At lower resolutions from 3.3 to 4.5 Å, when an AU contains multiple molecules, an electron density averaging method known as noncrystallographic symmetry (NCS) averaging has been used to overcome the lower-resolution problem (41, 42). NCS averaging and B-factor sharpening are very powerful tools for obtaining atomic resolution electron density. In our case, the alpha-helix was initially tube-shaped on the normal 2Fo-Fc map, but after 12-fold NCS averaging between the 12 HAs, as well as the 12 Fabs and B-factor sharpening, the electron density of side chains appeared clearly. We finally achieved substantial map improvement up to atomic resolution level (Fig. 6B to E). Positive density for N-linked glycans was observed at five of the six predicted sites on HA, and a total of 20 sugar residues were built. The overall structure of Aic68 HA in the complex is similar to that of the H3 starting model (Protein Data Bank [PDB] accession code

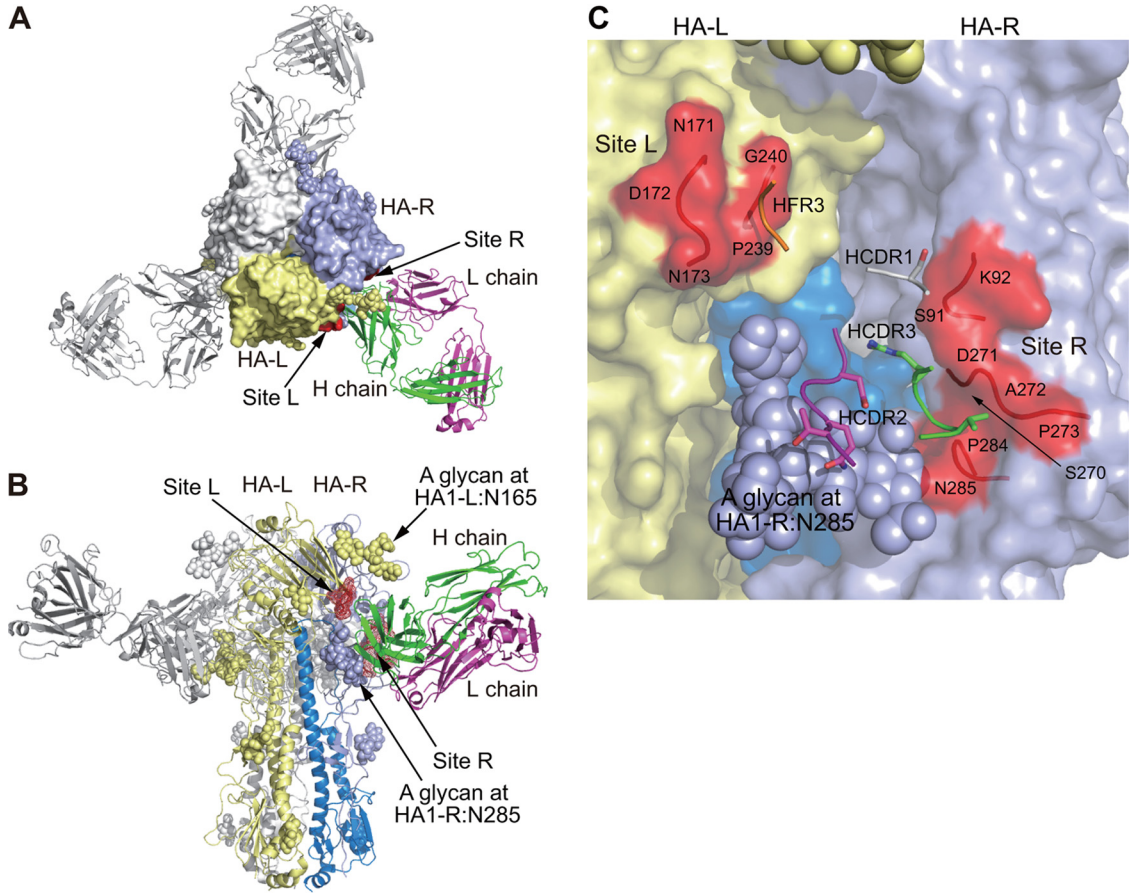

FIG 7 Crystal structure of F005-126 Fab in complex with Aic68/HA. (A and B) Top and side views, respectively, of the crystal structure. Trimeric HAs are depicted in a surface representation (A) and by ribbons (B). HA-L, HA1-R, HA2-R, and an HA in an HA trimer are indicated in light yellow, lavender, blue, and white, respectively. Sites L and R are shown in red. F005-126 Fabs are shown as ribbons. One Fab is colored. The H and L chains are green and magenta, respectively. Glycans are depicted as spheres. (C) Closeup view of sites L and R. A glycan at Asn285 in HA1-R is depicted as lavender spheres. CDR1, CDR2, CDR3, and FR3 of the H chain are depicted as wire frames in gray, magenta, green, and orange, respectively. Sites L and R are indicated in red.

1HA0). The F005-126 Fab spans a cleft formed by two neighboring globular heads in an HA trimer and cross-links them (HA monomer at the left side [HA-L] and that at the right side [HA-R] of an HA trimer in the side view). Three Fabs bind to the HA trimer in the same manner (Fig. 7A and B). The contact region is located in the space between two glycans linked to Asn165 in HA1-L and Asn285 in HA1-R. Although the Ab does not make contact with the glycan at Asn165, it directly interacts with HA at three locations, site L (residues 171 to 173, 239, and 240) and site R (residues 91, 92, 270 to 273, 284, and 285) and the glycan linked to Asn285 (Fig. 7C, 8A, and 8B).

Amino acid residues in four distinct regions of the Ab—CDR1, -2, and -3 plus framework region 3 (FR3) in the V_H domain—are involved in binding to HA. The V_L domain does not directly contribute to binding. At site L, a loop composed of Thr73, Gly74, and Thr75 in FR3 of the V_H domain is inserted into a narrow groove formed by two hairpin loops of HA1-L, residues 170 to 176 and residues 238 to 241 (Fig. 7C). These three amino acids in FR3 form van der Waals (VDW) contacts mainly with the main chain of the amino acids in site L (Fig. 9A). At site R, Val98, Arg99, Gly100, and Val100a in CDR3 are inserted into a narrow space formed by two loops of HA1 (residues 269 to 273 and residues 283 to 286) and the glycan linked to HA1-R:Asn285. These four amino acid residues in CDR3 make VDW contacts with the main chain of the amino acids in site R. In addition to the VDW contacts, two hydrogen bonds are formed between the C=O bond of Val98 and the side chain of HA1-R:Asp271, as well as between the main chain NH of Arg99 and the side chain of HA1-R:Asp271 (Fig. 9B). Furthermore, Ser31 in CDR1 forms hydrogen bonds with HA1-R:Ser91. Site L is located at the rim of a cleft formed by HA monomers in a receptor-binding subdomain, and residues 91, 92, and 270 to 273 in site R are located at the rim of the cleft in a vestigial esterase subdomain. Tyr53, Asp54, Gly55, Gln56, and Thr57 in CDR2 and Arg99, Gly100, and Val100a in CDR3 form long-range VDW contacts and hydrogen bonds with the glycan at HA1-R:Asn285 (Fig. 9B and C). The crystal structure improved by NCS averaging indicates that F005-126 H chain forms 9 hydrogen bonds with the glycan at Asn285 in HA1: the C=O of Asp54, Gly55, Arg99, and Gly100 with MAN5 (O2), BMA3 (O2), NAG1 (O6), and NAG1 (O5), respectively; the side chains of Asp54 (OD1) and Thr57 (OG1) with NAG2 (O7) and MAN4 (O6), respectively; the side chain of Gln56 (OE1) with BMA3 (O2), as well as NAG2 (O4); and the side chain of Gln56 (NE2) with NAG2 (O4) (Fig. 9B). A total area of 1,084 $Å^2$ for HA is buried at the contact surface. Sixty percentage of the area arises from the peptide portion, and 40% of the area arises from the glycan. The ratio of surface areas

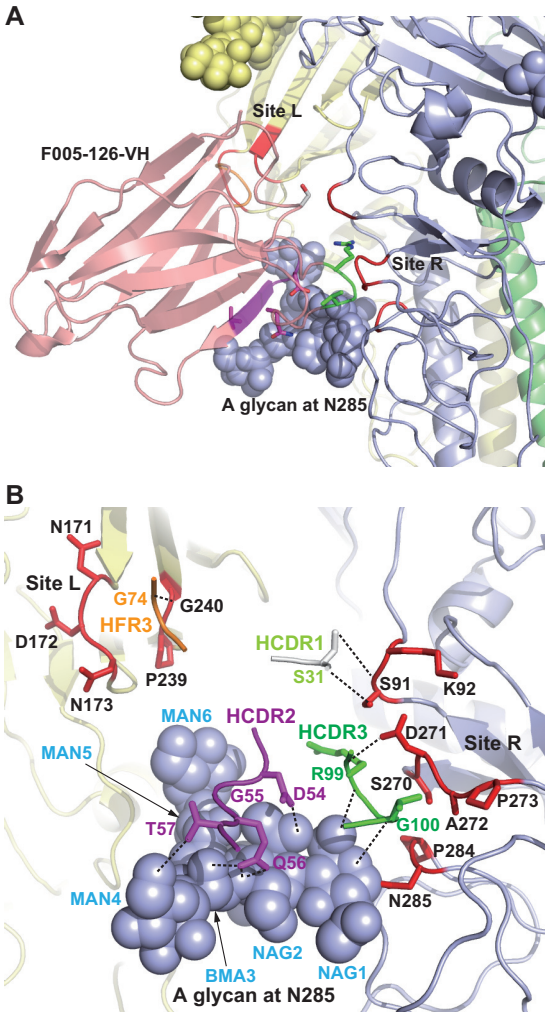

FIG 8 Crystal structure of F005-126 Fab in complex with Aic68/HA. (A and B) Epitopes on HA recognized by F005-126 are shown. In panel B, putative hydrogen bonds are depicted as broken lines.

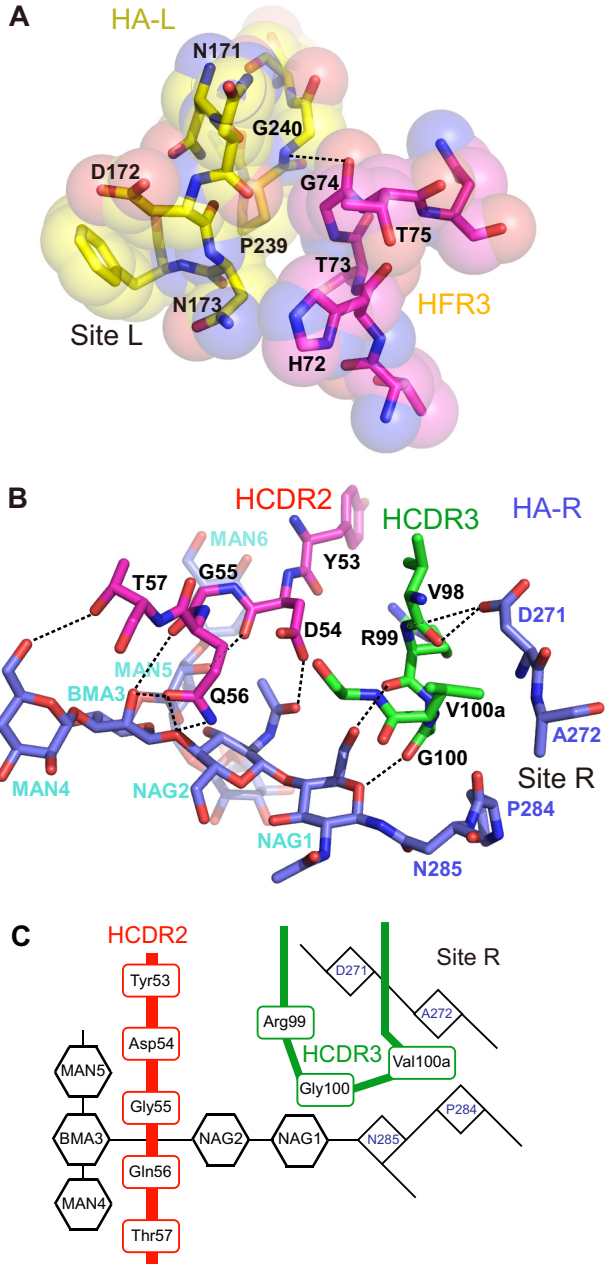

FIG 9 Interactions between F005-126 Fab and Aic68/HA in the crystal. (A) Interactions between site L and FR3 of the H chain are shown. (B) Interactions among site R, the glycan at HA1-R:Asn285, HCDR2 and HCDR3 are shown. *N*-acetyl-D-glucosamine, α-D-mannose, and β-D-mannose are abbreviated as NAG, MAN, and BMA, respectively. Putative hydrogen bonds are depicted as broken lines. (C) The interactions in Fig. 7B are schematically depicted.

covered by the above three components, site L, site R, and the glycan, is 17:43:40. The amino acids involved in the interaction between F005-126 and HA are marked in color in Fig. 1A and S1 in the supplemental material.

Inhibition of low-pH-induced structural change in HA by F005-126. How does F005-126 mediate virus-neutralization? Neutralizing Abs prevent binding of HA to sialic acid or prevent low-pH-induced structural change of HA, although there may be additional unidentified mechanisms. Judging from the location of the epitope, it is unlikely that F005-126 would prevent the binding of HA to sialic acid. In fact, it did not have HI activity. Traditionally, structural changes in HA have been examined by susceptibility to trypsin (47). Trypsin cleavage sites at Lys27 and Arg224 of H3 HA are not accessible in the neutral pH structure, but when the conformational change occurs at low pH, HA becomes susceptible to trypsin digestion. This trypsin susceptibility assay has previously been used to examine the activity of MAbs (8, 12, 13, 15, 45). We utilized this assay and examined the ability of F005-126 to prevent the conformational change in HA at low pH. As shown in Fig. 10A, F005-126 prevents conversion of HA from the protease-resistant to protease-susceptible form at pH 5.0. Thus, we concluded that F005-126 neutralizes influenza viruses by preventing low-pH-induced conformational change in HA.

DISCUSSION

The present study revealed the following. (i) A neutralizing epitope shared by H3 subtype viruses from 1968 to 2004 tested is present at the side of the globular head of HA. (ii) While a few amino acids in the epitope are not conserved among H3 viruses,

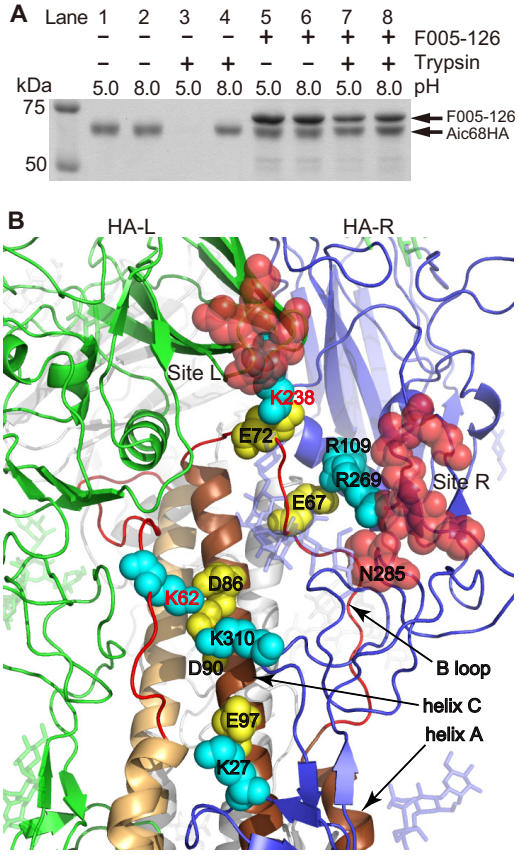

FIG 10 Inhibition of the low-pH-induced conformational changes by binding of F005-126 to HA1s. (A) HA was digested by trypsin after incubation at low pH (lane 3), but F005-126 prevented the low-pH-induced conformational change and thus rendered HA resistant to trypsin (lane 7). (B) HA1-L, HA2-L, HA1-R, and HA2-R are depicted in green, light brown, blue, and dark brown, respectively, except for the B loop. The B loops in HA2-L and HA2-R are depicted in red. The following residues in sites L and R are shown as red spheres: residues 171 to 173, 239, and 240 in HA1-L and residues 91, 92, 270 to 273, 284, and 285 in HA1-R. Glycans are depicted as sticks. The following amino acid residues are shown as spheres: K238 in HA1-L (cyan); K27, R109, R269, and K310 in HA1-R (cyan); K62 in HA2-L (cyan); and E67, E72, D86, D90, and E97 in HA2-R (yellow). [HA1-R:R109]-[HA2-R:E67]-[HA1-R:R269] in H3N2 make salt bridges (57). The crystal structure of H3N2 HA also shows the other putative salt bridges made by the following amino acids: [HA1-L:K238]-[HA2-R:E72], [HA2-L:K62]-[HA2-R:D86D90]-[HA1-R:K310], and [HA1-R:K27]-[HA2-R:E97].

the main chain of the peptide contributes to the formation of VDW contacts. (iii) The glycan linked to Asn is directly involved in HA-Ab complex formation. (iv) The epitope is distributed in two neighboring HA monomers in an HA trimer. (v) F005-126 spans a cleft formed by the two globular heads and cross-links them. (vi) Finally, F005-126 inhibits low-pH-induced structural change in HA. The structure of the HA-Ab complex revealed by X-ray analysis is consistent with the experimental findings, although the presence of site L in the epitope was only revealed by the X-ray analysis. X-ray analysis revealed that the sugar portion linked to Asn285 largely contributed to HA-Ab interaction. The role of glycans in HA remains undefined, and removal of individual glycans has no effect on the folding and intracellular transport of HAs (48). However, mutant HAs having less than five glycans in H3N2 HA form intracellular aggregates (48). Although a variant

TABLE 3 Conservation of 15 amino acids, including sites L and R in 5668 H3 HAs

Aic68/HA	Site (frequency[a] [%])
Ser91	5642 (99.5)
Lys92	5319 (93.8)
Asn171	5656 (99.8)
Asp172	485 (8.6)
Asn173	251 (4.4)
Pro239	5662 (99.9)
Gly240	5667 (100.0)
Ser270	5668 (100.0)
Asp271	5522 (97.4)
Ala272	5651 (99.7)
Pro273	5527 (97.5)
Pro284	5659 (99.8)
Asn285	5665 (99.9)
Gly286	5668 (100.0)
Ser287	5667 (100.0)

[a] Numbers of HAs with the same amino acid as that of Aic68/HA in 5668 HAs.

virus, Aic68N285Y, which lacks the glycan at Asn285 was isolated in the present study, the glycan at Asn285 is conserved in circulating H3N2 viruses. We surveyed 5668 sequences of H3 HAs from 1968 to 2012 in the National Center for Biotechnology Information FLU database and found only four deglycosylated variants: an S287N mutant (A/New York/715/1994 [H3N2], GenBank accession no. ABG47950), two N285D mutants (A/Finland/338/1995 [H3N2], AFH00351; A/New York/503/1997 [H3N2], ABB77853), and a N285S mutant (A/New York/412/2002 [H3N2], ABA42412).

In addition to the conserved glycan at Asn285, F005-126 bound to two peptide portions, sites L and R. We investigated the conservation of 15 amino acids in Aic68/HA, including these sites in the 5668 H3 HAs. Amino acid residues 91, 92, 171, 239, 240, 270 to 273, and 284 to 287 are conserved, whereas residues 172 and 173 at site L are variable among H3N2 viruses (Table 3). X-ray analysis

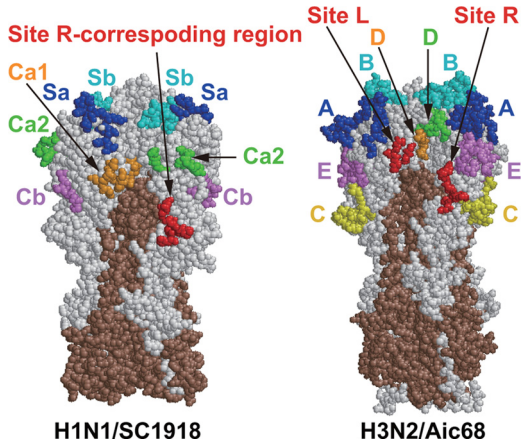

FIG 11 Antigenic sites in HA trimers of H1N1/SC1918 and H3N2/Aic68. HA1s and HA2s in HA trimers are white and brown, respectively. (Left) Antigenic sites Sa (blue), Sb (cyan), Ca1 (orange), Ca2 (green), and Cb (violet) in two of three HAs from H1N1/SC1918 are indicated in colors, and a region corresponding to site R is red. (Right) Antigenic sites A (blue), B (cyan), C (yellow), D in the left side of HA (orange), D in the right side of HA (green), and E (violet) in two of three HAs from H3N2/Aic68 are colored as indicated, and sites L and R are red.

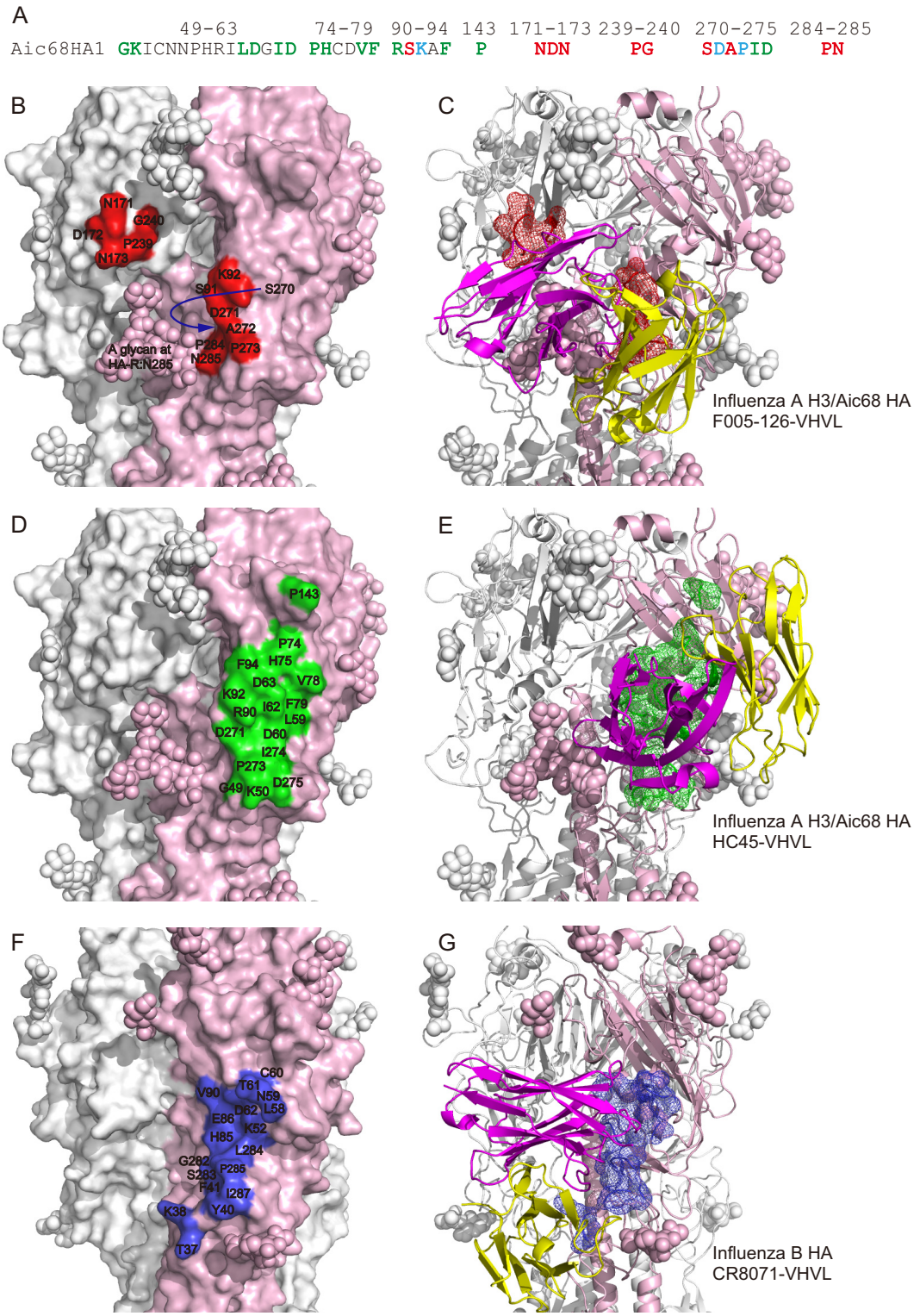

FIG 12 Comparison of epitopes recognized by F005-126, HC45, and CR8071. (A) The amino acid sequences of Aic68 HA recognized by F005-126 (red), HC45 (green), and both Abs (cyan) are colored as indicated. (B to G) An HA protomer in each HA trimer is light pink. The epitopes in HA of Aic68 recognized by F005-126 (B and C) and HC45 (PDB ID 1QFU) (D and E) are indicated in red and green, respectively. The amino acid numbers in HA of influenza virus A Aic68 strain are shown in panels B and D. The epitope in HA of influenza virus B recognized by CR8071 (PDB ID 4FQK) is blue (F and G). The amino acid numbers in HA of influenza virus B, which do not correspond to that in HA of influenza virus A H3, are shown. The VH and VL domains are magenta and yellow, respectively (C, E, and G).

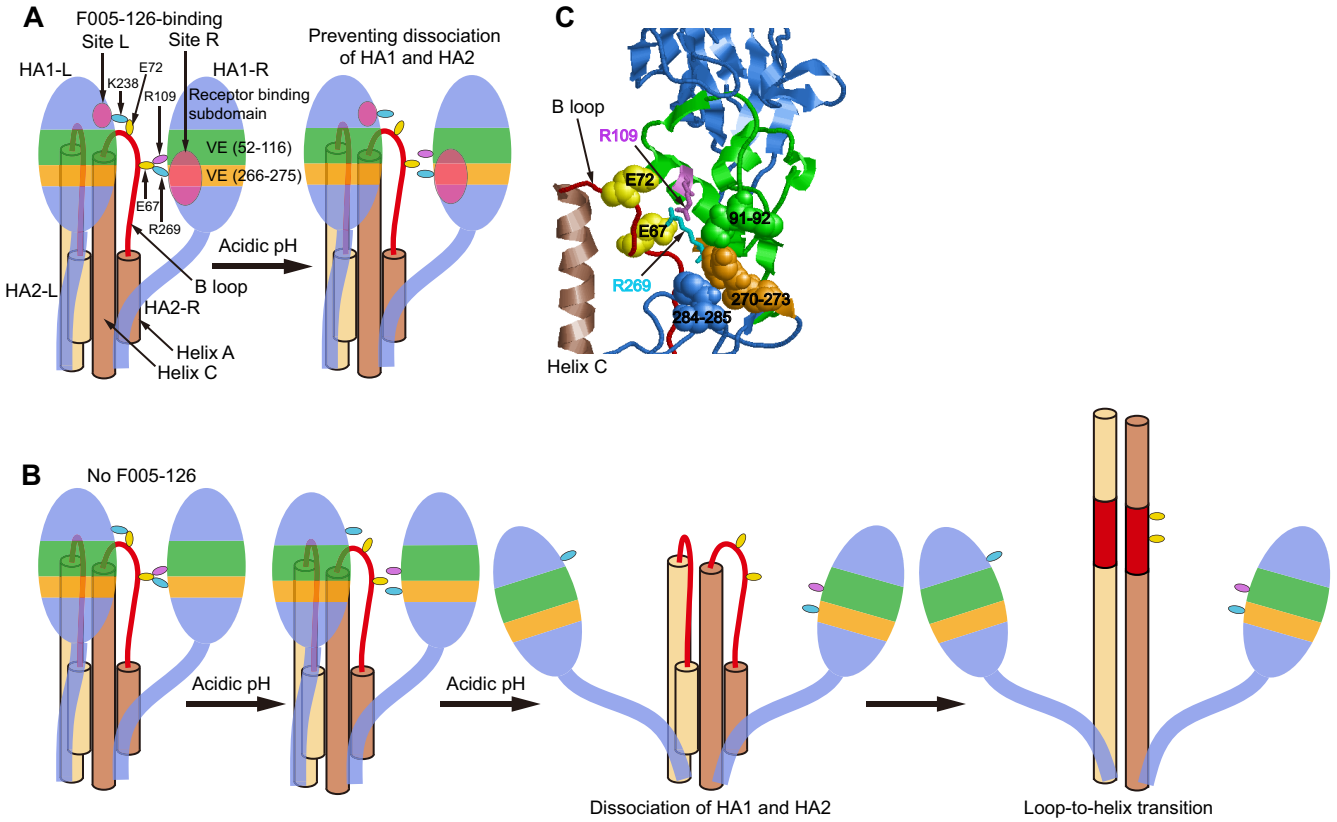

FIG 13 Illustrations on a proposed mechanism for preventing dissociation of HA1 and HA2 by F005-126. (A and B) HA1, helix A, B loop and helix C in two HA protomers in an HA trimer are illustrated. A vestigial esterase (VE) subdomain is green (residues 52 to 116) and orange (residues 266 to 275), and other regions in HA1 are blue. Arg109 and Arg269 are violet and cyan, respectively. Glu67 and Glu72 in B loop are yellow. Sites L and R are indicated in magenta. Under the low-pH condition, initially, part of the salt bridges are broken, and finally, the salt bridges are completely broken. When F005-126 binds to HA, dissociation does not occur at low pH, even if the salt bridges are broken (A). Dissociation of HA1 and HA2 occurs at low pH without F005-126 (B). (C) Arg109 and Arg269 are depicted as sticks in violet and cyan, respectively. Glu67 and Glu72 in B loop are depicted as surface representation in yellow. Residues 91, 92, 270 to 273, 284, and 285 in site R are depicted as surface representations.

reveals that F005-126 mainly forms VDW contacts with the main chain of the amino acid residues in site L, except a hydrogen bond with Gly240. Even at site R, the VDW contacts with the main chain of the amino acids make a major contribution to the recognition of HA. In addition, F005-126 forms few hydrogen bonds with side chains of conserved amino acids at site R. These characteristics of HA recognition by F005-126 explain the broad neutralization activity of this Ab against H3 viruses and its resistance to escape mutations of HA. On the other hand, F005-126 has diverse neutralization activities for 12 tested H3 strains, despite the recognition of conserved amino acids other than residues 172 and 173. Simple correlations between the sequence diversity of residues 172 and 173 and the diverse neutralization activities were not seen (Table 1 and see Fig. S1 in the supplemental material). Thus, it is unlikely that the diversity of residues 172 and 173 are the main reason for the diverse activities. Numerous mutations are introduced in HA1. Mutations in amino acids that are not directly involved in binding of F005-126 to HA may affect the 3D structure of HA or prevent binding. Some of the broadly neutralizing Abs against HA head reported by other groups also have diverse activities for various H1 strains (16, 19, 20) and H3 strains (21, 22), despite recognition of highly conserved amino acids.

F005-126 recognizes a distinct epitope from other broadly neutralizing Abs that bind to the globular head (15–23). Although F005-126 recognizes two peptide portions (site L and site R) and a glycan linked to Asn285, the glycan has not been identified as the neutralizing epitope to date. Sites L and R do not include antigenic sites A to E (see Fig. S1 in the supplemental material). While site L corresponds to site Ca_1 identified in H1 HA (see Fig. S1 in the supplemental material and Fig. 11) (4, 49), site R partly overlaps with the epitope recognized by MAb HC45. The epitope recognized by F005-126 is distributed to neighboring two HA monomers. It is possible that Abs that recognize Ca_1 and Ca_2 as well as site D have characteristics similar to F005-126 (Fig. 11).

Although the epitope recognized by MAb HC45 partly includes site R, as indicated in Fig. 12A, B, and D, HC45 inhibits the binding of viruses to cells (50, 51). The difference in function between F005-126 and HC45 may be caused by the distinct orientation of the Abs toward the binding sites in HAs, as indicated in Fig. 12C and E. Moreover, HC45 is not a broadly neutralizing Ab. The epitope of CR8071, which is an MAb against HA of influenza virus B, is located near a cleft formed by neighboring HAs in an HA trimer, which is near the region corresponding to site R in H3 HA (Fig. 12F and G) (15). However, CR8071 showed no HI activity and did not prevent conformational changes in HA at low pH.

There is an Ab, HC63, which cross-links the globular heads of two neighboring HA monomers. It prevents the conformational changes in HA induced by low pH, as well as F005-126 (45). The epitope recognized by HC63 is adjacent to the sialic acid-binding site. HC63 binds to HAs from 1968 to 1982 strains (52), although it is unknown whether the Ab binds to HA from 1983 to recent years. It has been suggested that HC63 neutralizes influenza viruses mainly by preventing receptor binding and that the prevention of structural change does not make a major contribution to neutralization (51).

Neutralizing Abs that prevent the structural changes in HA generally bind to the HA stem. They also have broad neutralization activity. Although the epitopes recognized by these Abs are largely different between 1-69V_H-encoding Abs and others, they are able to directly prevent a loop-to-helix transition of an interhelical loop (B loop) between helixes A and C by binding of the Ab to HA2 in the stem region. Since the loop-to-helix transition of the B loop is thermodynamically favorable and is not a low-pH-dependent process, the native structure of HA should be trapped in a metastable state (53–55). For stabilization, the HA1 subunit acts as a clamp to keep the B loop in HA2 in its metastable prefusion state at neutral pH (56). Salt bridges located between HA1 and HA2 within a monomer (intramonomer) and between neighboring HA monomers (intermonomer) play crucial roles in stabilizing the native HA form (57). The protonation of several amino acid residues in HA at low pH could induce destabilization of the native form by destruction of salt bridges and/or ionic repulsion caused by increases in net positive charge in HA1 (57, 58). Figure 8B indicates the relative location of site L, site R, and the asparagine at residue 285 that form the epitope for F005-126, as well as helix A, the B loop, and helix C. It also shows the location of five salt bridges predicted from the crystal structure of HA and described in a previous paper (57). Among these, two salt bridges, "[HA1-L:Lys238]-[HA2-R:Glu72]" and "[HA1-R:Arg109]-[HA2-R:Glu67]-[HA1-R:Arg269]," are located near sites L and R, respectively. Since F005-126 cross-links the neighboring HA monomers through binding to site L and site R, it will be able to maintain their association as paste, even if amino acids in the salt bridges are protonated. A proposed mechanism for preventing the dissociation of HA1 and HA2 by F005-126 is illustrated in Fig. 13. In addition, binding of F005-126 to a vestigial esterase (VE) subdomain, in which site R is located, may be related to prevention of conformational changes in HA. A mouse Ab, H5M9, recognizing an epitope including the VE domain in H5 HA prevents the conformational changes in HA, although the mechanisms for prevention remain unknown (59). In the case of H2 HA, low pH induces large deformation of the VE domain, and the domain serves as the relative flexible linker between the rigid receptor-binding domain and F′ fusion subdomain (56). F005-126 may prevent deformation of the VE domain by binding to site R, which may partly contribute to preventing the low-pH-induced conformational changes in HA. Neutralizing Abs, which cross-link two HA heads and prevent conformational changes, such as HC63 and F005-126, are rarely reported to date. It should be examined whether immunogenicity of such epitopes is strong enough to frequently induce antibody production in humans.

ACKNOWLEDGMENTS

We are grateful to Tadayuki Yamaguchi for sample preparation, Noriko Handa for data collection, and the staff of the SPring-8 BL41XU beamline for their assistance.

This study was supported in part by a grant-in-aid for the 21st Century Center of Excellence program of Fujita Health University from the Ministry of Education, Culture, Sports, Science, and Technology (MEXT) of Japan; a grant for Research on Pharmaceutical and Medical Safety from the Ministry of Health, Labor, and Welfare of Japan; a grant from the Research Foundation for Microbial Diseases, Osaka University; and the Targeted Proteins Research Program of MEXT.

REFERENCES

1. **Skehel JJ, Wiley DC.** 2000. Receptor binding and membrane fusion in virus entry: the influenza hemagglutinin. Annu. Rev. Biochem. **69:**531–569. http://dx.doi.org/10.1146/annurev.biochem.69.1.531.
2. **Wiley DC, Wilson IA, Skehel JJ.** 1981. Structural identification of the antibody-binding sites of Hong Kong influenza haemagglutinin and their involvement in antigenic variation. Nature **289:**373–378. http://dx.doi.org/10.1038/289373a0.
3. **Underwood PA.** 1982. Mapping of antigenic changes in the haemagglutinin of Hong Kong influenza (H3N2) strains using a large panel of monoclonal antibodies. J. Gen. Virol. **62:**153–169. http://dx.doi.org/10.1099/0022-1317-62-1-153.
4. **Caton AJ, Brownlee GG, Yewdell JW, Gerhard W.** 1982. The antigenic structure of the influenza virus A/PR/8/34 hemagglutinin (H1 subtype). Cell **31:**417–427. http://dx.doi.org/10.1016/0092-8674(82)90135-0.
5. **Salzberg S.** 2008. The contents of the syringe. Nature **454:**160–161. http://dx.doi.org/10.1038/454160a.
6. **Okuno Y, Isegawa Y, Sasao F, Ueda S.** 1993. A common neutralizing epitope conserved between the hemagglutinins of influenza A virus H1 and H2 strains. J. Virol. **67:**2552–2558.
7. **Smirnov YA, Lipatov AS, Gitelman AK, Okuno Y, Van Beek R, Osterhaus AD, Claas EC.** 1999. An epitope shared by the hemagglutinins of H1, H2, H5, and H6 subtypes of influenza A virus. Acta Virol. **43:**237–244.
8. **Dreyfus C, Ekiert DC, Wilson IA.** 2013. Structure of a classical broadly neutralizing stem antibody in complex with a pandemic H2 influenza virus hemagglutinin. J. Virol. **87:**7149–7154. http://dx.doi.org/10.1128/JVI.02975-12.
9. **Kashyap AK, Steel J, Oner AF, Dillon MA, Swale RE, Wall KM, Perry KJ, Faynboym A, Ilhan M, Horowitz M, Horowitz L, Palese P, Bhatt RR, Lerner RA.** 2008. Combinatorial antibody libraries from survivors of the Turkish H5N1 avian influenza outbreak reveal virus neutralization strategies. Proc. Natl. Acad. Sci. U. S. A. **105:**5986–5991. http://dx.doi.org/10.1073/pnas.0801367105.
10. **Throsby M, van den Brink E, Jongeneelen M, Poon LL, Alard P, Cornelissen L, Bakker A, Cox F, van Deventer E, Guan Y, Cinatl J, ter Meulen J, Lasters I, Carsetti R, Peiris M, de Kruif J, Goudsmit J.** 2008. Heterosubtypic neutralizing monoclonal antibodies cross-protective against H5N1 and H1N1 recovered from human IgM+ memory B cells. PLoS One **3:**e3942. http://dx.doi.org/10.1371/journal.pone.0003942.
11. **Sui J, Hwang WC, Perez S, Wei G, Aird D, Chen LM, Santelli E, Stec B, Cadwell G, Ali M, Wan H, Murakami A, Yammanuru A, Han T, Cox NJ, Bankston LA, Donis RO, Liddington RC, Marasco WA.** 2009. Structural and functional bases for broad-spectrum neutralization of avian and human influenza A viruses. Nat. Struct. Mol. Biol. **16:**265–273. http://dx.doi.org/10.1038/nsmb.1566.
12. **Ekiert DC, Bhabha G, Elsliger MA, Friesen RH, Jongeneelen M, Throsby M, Goudsmit J, Wilson IA.** 2009. Antibody recognition of a highly conserved influenza virus epitope. Science **324:**246–251. http://dx.doi.org/10.1126/science.1171491.
13. **Ekiert DC, Friesen RH, Bhabha G, Kwaks T, Jongeneelen M, Yu W, Ophorst C, Cox F, Korse HJ, Brandenburg B, Vogels R, Brakenhoff JP, Kompier R, Koldijk MH, Cornelissen LA, Poon LL, Peiris M, Koudstaal W, Wilson IA, Goudsmit J.** 2011. A highly conserved neutralizing epitope on group 2 influenza A viruses. Science **333:**843–850. http://dx.doi.org/10.1126/science.1204839.
14. **Corti D, Voss J, Gamblin SJ, Codoni G, Macagno A, Jarrossay D, Vachieri SG, Pinna D, Minola A, Vanzetta F, Silacci C, Fernandez-Rodriguez BM, Agatic G, Bianchi S, Giacchetto-Sasselli I, Calder L, Sallusto F, Collins P, Haire LF, Temperton N, Langedijk JP, Skehel JJ,**

Lanzavecchia A. 2011. A neutralizing antibody selected from plasma cells that binds to group 1 and group 2 influenza A hemagglutinins. Science **333:**850–856. http://dx.doi.org/10.1126/science.1205669.
15. **Dreyfus C, Laursen NS, Kwaks T, Zuijdgeest D, Khayat R, Ekiert DC, Lee JH, Metlagel Z, Bujny MV, Jongeneelen M, van der Vlugt R, Lamrani M, Korse HJ, Geelen E, Sahin Ö Sieuwerts M, Brakenhoff JP, Vogels R, Li OT, Poon LL, Peiris M, Koudstaal W, Ward AB, Wilson IA, Goudsmit J, Friesen RH.** 2012. Highly conserved protective epitopes on influenza B viruses. Science **337:**1343–1348. http://dx.doi.org/10.1126/science.1222908.
16. **Whittle JR, Zhang R, Khurana S, King LR, Manischewitz J, Golding H, Dormitzer PR, Haynes BF, Walter EB, Moody MA, Kepler TB, Liao HX, Harrison SC.** 2011. Broadly neutralizing human antibody that recognizes the receptor-binding pocket of influenza virus hemagglutinin. Proc. Natl. Acad. Sci. U. S. A. **108:**14216–14221. http://dx.doi.org/10.1073/pnas.1111497108.
17. **Schmidt AG, Xu H, Khan AR, O'Donnell T, Khurana S, King LR, Manischewitz J, Golding H, Suphaphiphat P, Carfi A, Settembre EC, Dormitzer PR, Kepler TB, Zhang R, Moody MA, Haynes BF, Liao HX, Shaw DE, Harrison SC.** 2013. Preconfiguration of the antigen-binding site during affinity maturation of a broadly neutralizing influenza virus antibody. Proc. Natl. Acad. Sci. U. S. A. **110:**264–269. http://dx.doi.org/10.1073/pnas.1218256109.
18. **Ekiert DC, Kashyap AK, Steel J, Rubrum A, Bhabha G, Khayat R, Lee JH, Dillon MA, O'Neil RE, Faynboym AM, Horowitz M, Horowitz L, Ward AB, Palese P, Webby R, Lerner RA, Bhatt RR, Wilson IA.** 2012. Cross-neutralization of influenza A viruses mediated by a single antibody loop. Nature **489:**526–532. http://dx.doi.org/10.1038/nature11414.
19. **Krause JC, Tsibane T, Tumpey TM, Huffman CJ, Basler CF, Crowe JE, Jr.** 2011. A broadly neutralizing monoclonal antibody that recognizes a conserved, novel epitope on the globular head of the influenza H1N1 virus hemagglutinin. J. Virol. **85:**10905–10908. http://dx.doi.org/10.1128/JVI.00700-11.
20. **Hong M, Lee PS, Hoffman RM, Zhu X, Krause JC, Laursen NS, Yoon SI, Song L, Tussey L, Crowe JE, Jr, Ward AB, Wilson IA.** 2013. Antibody recognition of the pandemic H1N1 influenza hemagglutinin receptor binding site. J. Virol. **87:**12471–12480. http://dx.doi.org/10.1128/JVI.01388-13.
21. **Yoshida R, Igarashi M, Ozaki H, Kishida N, Tomabechi D, Kida H, Ito K, Takada A.** 2009. Cross-protective potential of a novel monoclonal antibody directed against antigenic site B of the hemagglutinin of influenza A viruses. PLoS Pathog. **3:**e1000350. http://dx.doi.org/10.1371/journal.ppat.1000350.
22. **Lee PS, Yoshida R, Ekiert DC, Sakai N, Suzuki Y, Takada A, Wilson IA.** 2012. Heterosubtypic antibody recognition of the influenza virus hemagglutinin receptor binding site enhanced by avidity. Proc. Natl. Acad. Sci. U. S. A. **109:**17040–17045. http://dx.doi.org/10.1073/pnas.1212371109.
23. **Xu R, Krause JC, McBride R, Paulson JC, Crowe JE, Jr, Wilson IA.** 2013. A recurring motif for antibody recognition of the receptor-binding site of influenza hemagglutinin. Nat. Struct. Mol. Biol. **20:**363–370. http://dx.doi.org/10.1038/nsmb.2500.
24. **Ohshima N, Iba Y, Kubota-Koketsu R, Asano Y, Okuno Y, Kurosawa Y.** 2011. Naturally occurring antibodies in humans can neutralize a variety of influenza virus strains, including H3, H1, H2, and H5. J. Virol. **85:**11048–11057. http://dx.doi.org/10.1128/JVI.05397-11.
25. **Marks JD, Hoogenboom HR, Bonnert TP, McCafferty J, Griffiths AD, Winter G.** 1991. By-passing immunization. Human antibodies from V-gene libraries displayed on phage. J. Mol. Biol. **222:**581–597.
26. **Iba Y, Ito W, Kurosawa Y.** 1997. Expression vectors for the introduction of highly diverged sequences into the six complementarity-determining regions of an antibody. Gene **194:**35–46. http://dx.doi.org/10.1016/S0378-1119(97)00101-7.
27. **Morino K, Katsumi H, Akahori Y, Iba Y, Shinohara M, Ukai Y, Kohara Y, Kurosawa Y.** 2001. Antibody fusions with fluorescent proteins: a versatile regent for profiling protein expression. J. Immunol. Methods **257:**175–184. http://dx.doi.org/10.1016/S0022-1759(01)00462-8.
28. **Abhinandan KR, Martin AC.** 2008. Analysis and improvements to Kabat and structurally correct numbering of antibody variable domains. Mol. Immunol. **45:**3832–3839. http://dx.doi.org/10.1016/j.molimm.2008.05.022.
29. **Ito W, Kurosawa Y.** 1993. Development of an artificial antibody system with multiple valency using an Fv fragment fused to a fragment of protein A. J. Biol. Chem. **268:**20668–20675.
30. **Higo-Moriguchi K, Akahori Y, Iba Y, Kurosawa Y, Taniguchi K.** 2004. Isolation of human monoclonal antibodies that neutralize human rotavirus. J. Virol. **78:**3325–3332. http://dx.doi.org/10.1128/JVI.78.7.3325-3332.2004.
31. **Okuno Y, Tanaka K, Baba K, Maeda A, Kunita N, Ueda S.** 1990. Rapid focus reduction neutralization test of influenza A and B viruses in microtiter system. J. Clin. Microbiol. **28:**1308–1313.
32. **Nakagawa N, Kubota R, Nakagawa T, Okuno Y.** 2001. Antigenic variants with amino acid deletions clarify a neutralizing epitope specific for influenza B virus Victoria group strains. J. Gen. Virol. **82:**2169–2172.
33. **Ueda M, Maeda A, Nakagawa N, Kase T, Kubota R, Takamura H, Ohshima A, Okuno Y.** 1998. Application of subtype-specific monoclonal antibodies for rapid detection and identification of influenza A and B viruses. J. Clin. Microbiol. **36:**340–344.
34. **Okada J, Ohshima N, Kubota-Koketsu R, Ota S, Takase W, Azuma M, Iba Y, Nakagawa N, Yoshikawa T, Nakajima Y, Ishikawa T, Asano Y, Okuno Y, Kurosawa Y.** 2010. Monoclonal antibodies in man that neutralized H3N2 influenza viruses were classified in to three groups with distinct strain specificity: 1968-1973, 1977-1993 and 1997-2003. Virology **397:**322–330. http://dx.doi.org/10.1016/j.virol.2009.11.025.
35. **Okada J, Ohshima N, Kubota-Koketsu R, Iba Y, Ota S, Takase W, Yoshikawa T, Ishikawa T, Asano Y, Okuno Y, Kurosawa Y.** 2011. Localization of epitopes recognized by monoclonal antibodies that neutralized the H3N2 influenza viruses in man. J. Gen. Virol. **92:**326–335. http://dx.doi.org/10.1099/vir.0.026419-0.
36. **Kabsch W.** 1993. Automatic processing of rotation diffraction data from crystals of initially unknown symmetry and cell constants. J. Appl. Cryst. **26:**795–800. http://dx.doi.org/10.1107/S0021889893005588.
37. **Otwinowski ZO, Minor W.** 1997. Processing of X-ray diffraction data collected in oscillation mode. Methods Enzymol. **276:**307–326. http://dx.doi.org/10.1016/S0076-6879(97)76066-X.
38. **Chen J, Lee KH, Steinhauer DA, Stevens DJ, Skehel JJ, Wiley DC.** 1988. Structure of the hemagglutinin precursor cleavage site, a determinant of influenza pathogenicity and the origin of the labile conformation. Cell **95:**409–417.
39. **Fleury D, Daniels RS, Skehel JJ, Knossow M, Bizebard T.** 2000. Structural evidence for recognition of a single epitope by two distinct antibodies. Proteins **40:**572–578. http://dx.doi.org/10.1002/1097-0134(20000901)40:4<572::AID-PROT30>3.0.CO;2-N.
40. **Emsley P, Cowtan K.** 2004. Coot: model-building tools for molecular graphics. Acta Crystallogr. D Biol. Crystallogr. **60:**2126–2132. http://dx.doi.org/10.1107/S0907444904019158.
41. **Terwilliger TC.** 2000. Maximum-likelihood density modification. Acta Crystallogr. D Biol. Crystallogr. **56:**965–972. http://dx.doi.org/10.1107/S0907444900005072.
42. **Terwilliger TC.** 2002. Statistical density modification with non-crystallographic symmetry. Acta Crystallogr. D Biol. Crystallogr. **58:**2082–2086. http://dx.doi.org/10.1107/S0907444902016360.
43. **Chen VB, Arendall WB 3rd, Headd JJ, Keedy DA, Immormino RM, Kapral GJ, Murray LW, Richardson JS, Richardson DC.** 2010. MolProbity: all-atom structure validation for macromolecular crystallography. Acta Crystallogr. D Biol. Crystallogr. **66:**12–21. http://dx.doi.org/10.1107/S1744309109042018.
44. **Connolly ML.** 1983. Solvent-accessible surfaces of proteins and nucleic acids. J. Appl. Crystallogr. **221:**709–713.
45. **Barbey-Martin C, Gigant B, Bizebard T, Calder LJ, Wharton SA, Skehel JJ, Knossow M.** 2002. An antibody that prevents the hemagglutinin low pH fusogenic transition. Virology **294:**70–74. http://dx.doi.org/10.1006/viro.2001.1320.
46. **Wilson IA, Skehel JJ, Wiley DC.** 1981. Structure of the haemagglutinin membrane glycoprotein of influenza virus at 3 Å resolution. Nature **289:**366–373. http://dx.doi.org/10.1038/289366a0.
47. **Skehel JJ, Bayley PM, Brown EB, Martin SR, Waterfield MD, White JM, Wilson IA, Wiley DC.** 1982. Changes in the conformation of influenza virus hemagglutinin at the pH optimum of virus-mediated membrane fusion. Proc. Natl. Acad. Sci. U. S. A. **79:**968–972. http://dx.doi.org/10.1073/pnas.79.4.968.
48. **Gallagher PJ, Henneberry JM, Sambrook JF, Gething MJ.** 1992. Glycosylation requirements for intracellular transport and function of the hemagglutinin of influenza virus. J. Virol. **66:**7136–7145.
49. **Xu R, Ekiert DC, Krause JC, Hai R, Crowe JE, Jr, Wilson IA.** 2010. Structural basis of preexisting immunity to the 2009 H1N1 pandemic

influenza virus. Science **328:**357–360. http://dx.doi.org/10.1126/science.1186430.
50. **Fleury D, Barrère B, Bizebard T, Daniels RS, Skehel JJ, Knossow M.** 1999. A complex of influenza hemagglutinin with a neutralizing antibody that binds outside the virus receptor binding site. Nat. Struct. Biol. **6:**530–534. http://dx.doi.org/10.1038/9299.
51. **Knossow M, Gaudier M, Douglas A, Barrère B, Bizebard T, Barbey C, Gigant B, Skehel JJ.** 2002. Mechanism of neutralization of influenza virus infectivity by antibodies. Virology **302:**294–298. http://dx.doi.org/10.1006/viro.2002.1625.
52. **Daniels PS, Jeffries S, Yates P, Schild GC, Rogers GN, Paulson JC, Wharton SA, Douglas AR, Skehel JJ, Wiley DC.** 1987. The receptor-binding and membrane-fusion properties of influenza virus variants selected using anti-haemagglutinin monoclonal antibodies. EMBO J. **6:**1459–1465.
53. **Carr CM, Kim PS.** 1993. A spring-loaded mechanism for the conformational change of influenza hemagglutinin. Cell **73:**823–832. http://dx.doi.org/10.1016/0092-8674(93)90260-W.
54. **Bullough PA, Hughson FM, Skehel JJ, Wiley DC.** 1994. Structure of influenza haemagglutinin at the pH of membrane fusion. Nature **371:**37–43. http://dx.doi.org/10.1038/371037a0.
55. **Carr CM, Chaudhry C, Kim PS.** 1997. Influenza hemagglutinin is spring-loaded by a metastable native conformation. Proc. Natl. Acad. Sci. U. S. A. **94:**14306–14313. http://dx.doi.org/10.1073/pnas.94.26.14306.
56. **Xu R, Wilson IA.** 2011. Structural characterization of an early fusion intermediate of influenza virus hemagglutinin. J. Virol. **85:**5172–5182. http://dx.doi.org/10.1128/JVI.02430-10.
57. **Rachakonda PS, Veit M, Korte T, Ludwig K, Böttcher C, Huang Q, Schmidt MF, Herrmann A.** 2007. The relevance of salt bridges for the stability of the influenza virus hemagglutinin. FASEB J. **21:**995–1002. http://dx.doi.org/10.1096/fj.06-7052hyp.
58. **Huang Q, Opitz R, Knapp EW, Herrmann A.** 2002. Protonation and stability of the globular domain of influenza virus hemagglutinin. Biophys. J. **82:**1050–1058. http://dx.doi.org/10.1016/S0006-3495(02)75464-7.
59. **Zhu X, Guo YH, Jiang T, Wang YD, Chan KH, Li XF, Yu W, McBride R, Paulson JC, Yuen KY, Qin CF, Che XY, Wilson IA.** 2013. A unique and conserved neutralization epitope in H5N1 influenza viruses identified by a murine antibody against the A/goose/Guangdong/1/96 hemagglutinin. J. Virol. **87:**12619–12635. http://dx.doi.org/10.1128/JVI.01577-13.
60. **Karplus PA, Diederichs K.** 2012. Linking crystallographic model and data quality. Science **336:**1030–1033. http://dx.doi.org/10.1126/science.1218231.